

Selective coherent destruction of tunneling in a quantum-dot array

J. M. Villas-Bôas,^{1,2} Sergio E. Ulloa,¹ and Nelson Studart²

¹*Department of Physics and Astronomy, Nanoscale and Quantum Phenomena Institute, Ohio University, Athens, Ohio 45701-2979*

²*Departamento de Física, Universidade Federal de São Carlos, 13565-905, São Carlos, São Paulo, Brazil*

(Dated: October 30, 2018)

The coherent manipulation of quantum states is one of the main tasks required in quantum computation. In this paper we demonstrate that it is possible to control coherently the electronic position of a particle in a quantum-dot array. By tuning an external ac electric field we can selectively suppress the tunneling between dots, trapping the particle in a determined region of the array. The problem is treated non-perturbatively by a time-dependent Hamiltonian in the effective mass approximation and using Floquet theory. We find that the quasienergy spectrum exhibits crossings at certain field intensities that result in the selective suppression of tunneling.

PACS numbers: 78.67.Hc, 72.20.Ht, 73.40.Gk

Keywords: dynamic localization, quantum dot, tunneling, ac field

The search for a solid-state based quantum computer device has attracted a lot of interest in the physics community recently. The ability to manipulate a quantum state and measure it is one of the most important and pressing challenges to be addressed in real implementations. Fortunately great advances in this area have been achieved recently. A good example of that are the Rabi oscillations observed in exciton states of self-assembled quantum dots (QDs).^{1,2,3,4}

Our work here is based on the coherent destruction of tunneling (CDT) of a driven two-level system,^{5,6,7} in which the tunneling of one particle in a symmetric double well potential is suppressed for some special value of frequency and field intensity. We propose a system in which one can selectively suppress the tunneling between individual quantum dots tuned by the external ac electric field. This effect provides one with a different experimental handle to control a quantum mechanical system. By suitable variation of the frequency and applied ac field amplitude, one can precise the location of one electron in the multidot array. To demonstrate this effect, our model employs an effective mass nearest-neighbor tight-binding approximation (NNTB).^{8,9,10} The dynamics is analyzed using Floquet theory and the direct integration of the time-dependent Schrödinger equation.

The Hamiltonian for an electron in an array of identical QDs under a strong ac field within NNTB is written as

$$H = \sum_j T_e (a_{j+1}^\dagger a_j + h.c.) + \sum_j eFdja_j^\dagger a_j \cos(\omega t + \phi), \quad (1)$$

where T_e is the hopping matrix element, a_j^\dagger and a_j are, respectively, the electron creation and annihilation operator in the dot j , e is the electronic charge, F is the field intensity, d is the separation between dots, ω is the field frequency, and ϕ is the phase of the drive field. This phase, first thought to be a non-relevant factor, is in fact quite an important parameter in the CDT at smaller frequency, as we have recently shown.¹¹ Indeed, a phase $\phi = \pi/2$ produces a much better dynamic localization

than any other possible phase ϕ , and consequently it is our choice here.

Since H is periodic in time ($H(t) = H(t + \tau)$, where $\tau = 2\pi/\omega$ is the period) we can make use of the standard Floquet theory^{7,12} and write the solutions of the time-dependent Schrödinger equation as $\psi(t) = \exp(-i\varepsilon t/\hbar)u(t)$, where $u(t)$, the so-called Floquet state, is also periodic in time with the same period τ , and ε is the Floquet characteristic exponent or quasienergy, which can be obtained from the eigenvalue equation

$$\left(H - i\hbar \frac{\partial}{\partial t} \right) u(t) = \varepsilon u(t). \quad (2)$$

Note that this equation is similar to the time-independent Schrödinger equation with $\mathcal{H} = H - i\hbar \partial_t$ playing the role of a time-independent Hamiltonian. Using this analogy we can explore a combined dynamic parity operation: $z \rightarrow -z; t \rightarrow t + \tau/2$, under which the operator \mathcal{H} is invariant. As a consequence, each Floquet state is either even or odd under this operation.¹² Quasienergies of different “dynamic parity” may cross, while an avoided crossing is expected as a function of external parameters, such as the field intensity, for states with the same parity.

In a symmetric double QD the levels present strictly different parity, and they may exhibit crossings with field unless the symmetry is broken. If we vary the field intensity, and the quasienergy levels cross, a CDT is expected, since a splitting between levels comes from this inter-dot tunneling. This CDT result is well known in the high frequency limit, and it occurs at field values satisfying the zeroes of the Bessel function, $J_0(eFd/\hbar\omega) = 0$. As we have shown in Ref. 12, and extended by Creffield,¹³ CDT may also occur at lower frequency with decreasing degree of localization and at different intensities of the driven field. The dynamics of the system can be drastically different, depending on the numbers of dots. We note that for this effect to be observed, the frequency of the driven field cannot be excessively high, compared

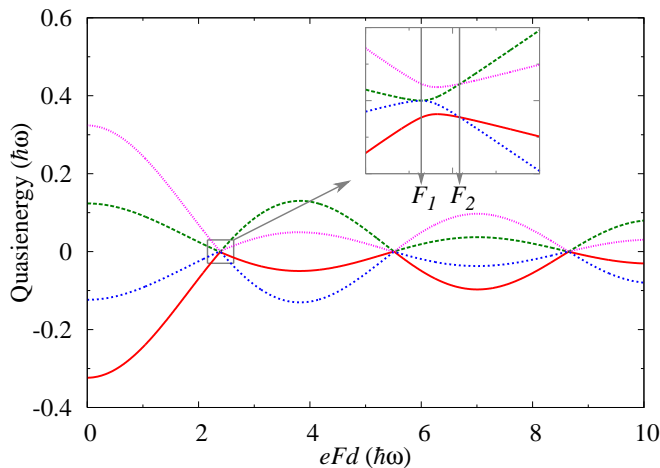


FIG. 1: (Color online) First Brillouin zone of quasienergies (in units of $\hbar\omega$) as function of ac field intensity ($eFd/\hbar\omega$), for $T_e/\hbar\omega = 0.2$. Inset shows amplification of collapse region, showing crossings and anticrossing that follow a definite pattern according to dynamical symmetries. The two vertical lines indicate field intensity F_1 and F_2 of pair crossings and are used later in numerical simulation.

with the tunneling probability between nearest dots, as otherwise the level splitting will be so small as to be unnoticeable. It should also be pointed out that in the limit of an infinite number of identical QDs the levels form a miniband with bandwidth of $4T_e$, and since there is an infinite number of levels in that range, they are infinitesimally separated, so that even at low frequencies the levels collapse at the zeroes of the Bessel function. Notice that the applicability of the NNTB in that limit system has some limitations.^{14,15,16} The system considered here has just a few QDs and we assume weak coupling between them, so that the NNTB can be applied with confidence. Notice also that we are considering a different kind of dynamic localization since we do not focus only in the probability to find the particle in the same initial state, but in a determined region of the dot array that may not be necessarily the initial localized state. In fact the particle stays confined to a determined multidot region of the array.

In our analysis, we focus on the dynamics of four QDs. However, we show that similar results can be obtained for other numbers of QDs as well. In Fig. 1 we show the quasienergy spectrum as a function of the field intensity for the ratio $T_e/\hbar\omega = 0.2$ exhibiting the strong dependence on field amplitude and the expected collapse of the spectrum near field values for which $J_0(eFd/\hbar\omega) = 0$. Notice however, as shown in the inset, that the region of the level collapse is in fact a region with several crossings and anticrossings following a well-defined pattern given by the dynamic parity. The two vertical lines in the inset are shown to indicate the two field values, F_1 and F_2 , where pairs of levels cross and are the choices of field intensity used for the numerical simulations below.

Our numerical simulation is done by direct integration

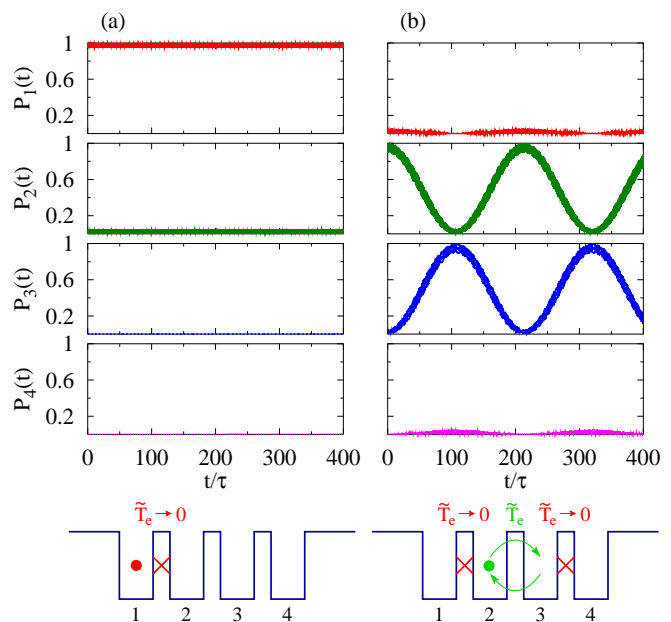


FIG. 2: (Color online) Time evolution of probability to find one particle in each one of the QDs in a four-dot array for $eF_1d/\hbar\omega \simeq 2.38$, and starting the system with the particle in: (a) dot 1, and (b) dot 2. Lower panel is a schematic representation of the dynamics of the system, as seen in the respective time evolution of the occupation probability of each dot. The full circle represents the position of the particle at time zero, crosses indicate the suppression of tunneling through that barrier and arrows indicate that tunneling is possible.

of the time-dependent Schrödinger equation and followed by calculations of the occupation probability for different choices of initial conditions. In Fig. 2(a) we show the time evolution of the system for the field intensity F_1 corresponding to the first vertical line in the inset of Fig. 1 ($eF_1d/\hbar\omega \simeq 2.38$), assuming that at time zero the particle is in the first QD. Notice that the particle is basically frozen in that dot, which means that for this choice of field we can effectively suppress the tunneling in the barrier between dots 1 and 2. This is what the bottom cartoon in Fig. 2 represents, where the cross in the barrier indicates that the tunneling is not allowed and that the effective interdot tunneling amplitude $\tilde{T}_e \rightarrow 0$. On the other hand, if we start the system with the particle in dot 2, Fig. 2(b) shows that the particle can tunnel back and forth between dots 2 and 3, while the effective tunneling is not only suppressed between dots 1 and 2, but between 3 and 4 also. The bottom panel represents the dynamics for this initial condition. We can then conclude that for this first choice of field intensity one can selectively block the tunneling of the electron through the outer barriers, so that the only open barrier for tunneling is the one in the middle.¹⁸

Let us now explore the second choice of field intensity F_2 , the second vertical line in the inset of Fig. 1, ($eF_2d/\hbar\omega \simeq 2.4$). This small but discernible tuning of

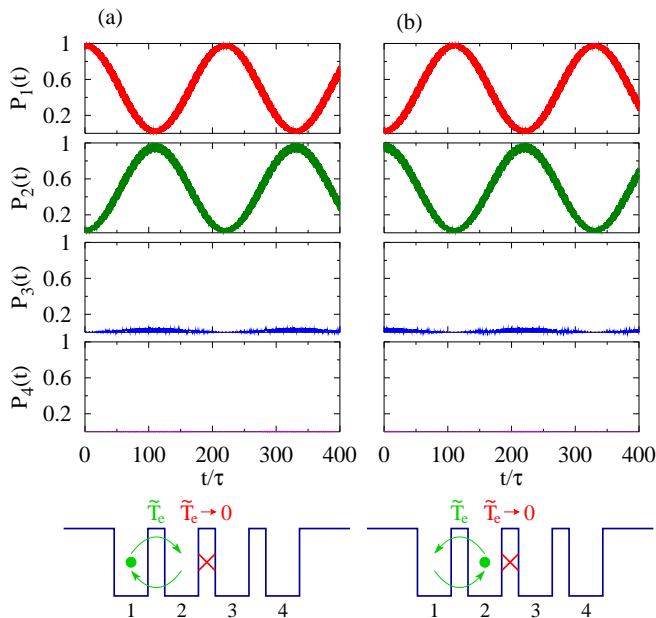


FIG. 3: (Color online) Time evolution of the probability to find a particle in one of the QDs for $eFd/\hbar\omega \simeq 2.40$, starting the system with the particle in: (a) dot 1, and (b) dot 2. Lower panel is a schematic representation of the dynamics. Here, the middle barrier tunneling is suppressed.

the field intensity yields a completely different result. At that point there are two crossings in the spectrum. In Fig. 3(a), we show the results when we start the system with the particle in dot 1, and in Fig. 3(b) starting in dot 2. The picture for both initial conditions does not change at all, except for a π -phase in the oscillation (that is provided by the initial state). The effective tunnelings can be summarized in the respective bottom panels of that figure, and we can see that now we can block the tunneling between dots 2 and 3. Similar behavior and conclusions are reached for initial conditions in either dot 3 or 4.

These examples represent an exciting result since by simply tuning the field intensity from F_1 to F_2 , one can choose which barrier is allowed or blocked for tunneling. Notice that this dot or site selectivity is achieved despite the ac field being applied to the entire structure, which suggests interesting applications. Notice, moreover, that the amount of field intensity needed to change this condition is relative to the frequency of the driving field, i.e., the ratio $T_e/\hbar\omega$. It is also interesting that the separation between the two tunneling suppressing fields is not a monotonic function of $T_e/\hbar\omega$. Figure 4(a) shows how these two crossing points change with the ratio $T_e/\hbar\omega$. The solid line shows the first crossing at field intensity F_1 , and the dashed line is the result for F_2 . Notice that in the high frequency regime (smaller ratio $T_e/\hbar\omega$) the crossings occur very close to each other and at field intensities satisfying the condition $J_0(eFd/\hbar\omega) = 0$. As a result, all barriers present a suppression of tunneling at the same

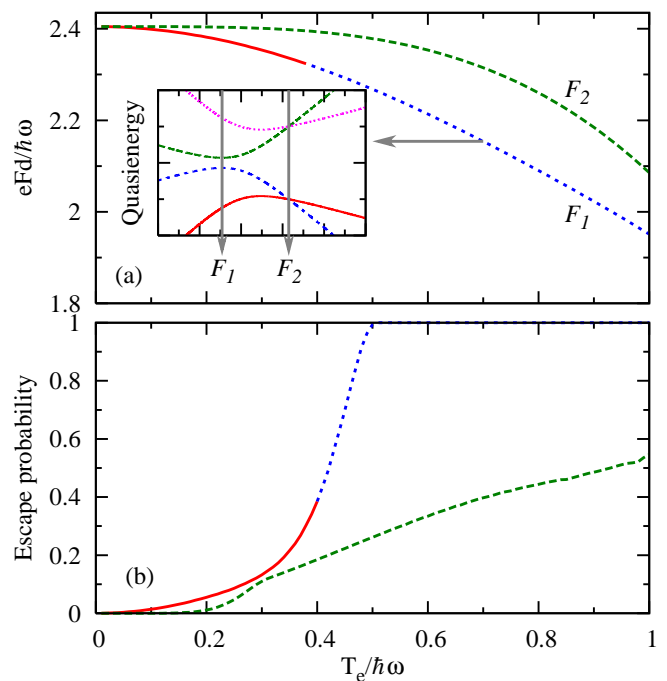


FIG. 4: (Color online) (a) Crossing in the collapse region as indicated by vertical lines in the inset of Fig. 1, as function of the ratio $T_e/\hbar\omega$. In the high frequency limit (lower ratio $T_e/\hbar\omega$) the crossings occur basically at the same point (zeroes of Bessel function). Inset shows amplification of quasienergy spectrum for $T_e/\hbar\omega = 0.7$. (b) Escape probability for a particle initially in one region of the quantum-dot array. Solid red line is for the equivalent first crossing and represents the escape probability of the QD 1, considering this dot as the initial condition. Dotted blue line continuation shows F_1 when the crossing disappears. Dashed green line is for the second crossing and represents escape probability of the first two QDs assuming that the system starts in QD 1.

value of field intensity in the high frequency regime.¹⁷ For lower frequencies and given T_e , the crossings become separated and different barriers are selectively closed at different fields. At even lower frequency $T_e/\hbar\omega \gtrsim 0.4$, the first crossing disappears (indicated by the dotted blue line continuation) as the coupling between quasienergy levels one and two, and two and four increases. This results in an effective gap in the quasienergy spectrum (see inset of Fig. 4(a) for $T_e/\hbar\omega = 0.7$) that basically kills the CDT for that value of field intensity and frequency.

To better understand how good is this CDT at values of field given by F_1 and F_2 we can monitor the maximum probability for the particle tunneling out of the region of dots we are considering (see Ref. 12). Lower values for this represent a good CDT. Figure 4(b) shows the escape probability for field intensities F_1 and F_2 provided by the crossings in Fig. 4(a), as function of the ratio $T_e/\hbar\omega$ (frequency). The solid line is the result for the first crossing F_1 , and is the escape probability out of dot 1, defined as the maximum value reached by $P_2 + P_3 + P_4$, assuming that the system starts with the particle in dot 1. The

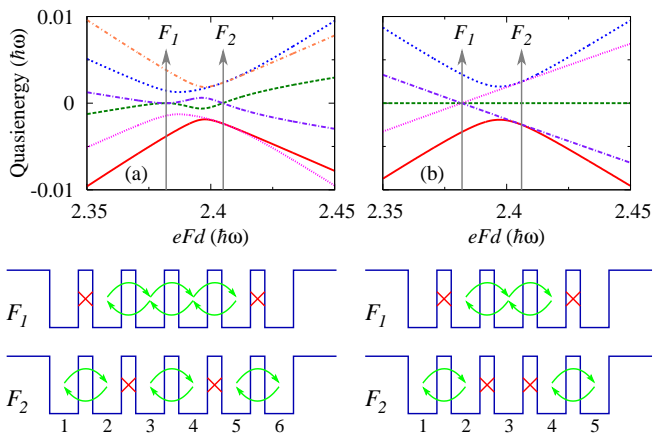


FIG. 5: (Color online) Collapse region of the first Brillouin zone of quasienergies (in units of $\hbar\omega$) as function of the ac field intensity ($eFd/\hbar\omega$), for $T_e/\hbar\omega = 0.2$ for: (a) an array of six QDs and (b) an array of five QDs. Lower cartoons are the schematic representation of the dynamic of the respective arrays of QDs at field intensity at crossing points given by F_1 and F_2 .

same result is clearly obtained if the system starts with the particle in dot 2 and one monitors the maximum probability to find it in dot 1. The dotted blue line that follows the solid red line in Fig. 4(b) is the result for field values F_1 at frequencies when there are no more crossing, but a gap in the quasienergy spectrum. Notice this goes to unity quickly as the effective tunneling becomes possible as a result of having a gap in the quasienergy spectrum. The dashed green line in Fig. 4(b) is the result for the second level crossing field F_2 , representing the escape probability of the dots 1 and 2 (since for this choice of field we suppress the tunneling between dots 2 and 3), which is the maximum value reached by $P_3 + P_4$ starting the system with the particle in either dots 1 or

2. Notice that for frequencies around $T_e/\hbar\omega \simeq 0.3$ the system still presents a good CDT for both crossings, and they occurs at field intensity with significant separation.

Our analysis was given for four QDs, but the same behavior can be obtained for other finite number of dots. The quasienergy spectrum presents two crossings, F_1 and F_2 , in the collapse region as we can see in Fig. 5(a) for six and (b) for five QDs, respectively. The first crossing F_1 basically suppresses the tunneling between dots 1 and 2, and between the two last QDs. This result is schematically represented in the bottom cartoons for F_1 for either five or six QDs. The second crossing in the spectrum, F_2 , suppress the tunneling between pairs of quantum dots, for example, in the six QDs cases, the tunneling between dots 2 and 3, and 4 and 5 as schematically represented in the lower bottom panel of Fig. 5(a). An interesting result appears for odd numbers of QDs, since in this case there is a different number of even and odd states. This fact allows for the dot in the middle to become a true trap for the particle, since tunneling in both directions can be suppressed. For example, the case of five QDs for the second crossing, F_2 , as schematically represented by the lower bottom cartoon of Fig. 5(d), suppress the tunneling between the dots 2 and 3, and 3 and 4. So, if we could start the system, or manipulate it, in a state localized in that dot and choose this value of field intensity (F_2) we could in principle trap the particle in the middle of the quantum-dot array.

In conclusion, we have shown that it is possible to suppress selectively the tunneling between quantum dots by a simple tuning from F_1 to F_2 , the intensity of an applied ac field. With this tool one could manipulate the position of the particle in a quantum-dot array, and assist in its initialization and control.

This work was partially supported by FAPESP, US DOE grant no. DE-FG02-91ER45334 and the CMSS Program at Ohio University.

¹ T. H. Stievater, Xiaoqin Li, D. G. Steel, D. Gammon, D. S. Katzer, D. Park, C. Piermarocchi, and L. J. Sham, *Phys. Rev. Lett.* **87**, 133603 (2001).
² H. Kamada, H. Gotoh, J. Temmyo, T. Takagahara, and H. Ando, *Phys. Rev. Lett.* **87**, 246401 (2001).
³ H. Htoon, T. Takagahara, D. Kulik, O. Baklenov, A. L. Holmes Jr., and C. K. Shih, *Phys. Rev. Lett.* **88**, 087401 (2002).
⁴ A. Zrenner, E. Beham, S. Stuffer, F. Findeis, M. Bichler, and G. Abstreiter, *Nature (London)* **418**, 612 (2002).
⁵ F. Grossmann, T. Dittrich, P. Jung, and P. Hänggi, *Phys. Rev. Lett.* **67**, 516 (1991).
⁶ R. Bavli and H. Metiu, *Phys. Rev. A* **47**, 3299 (1993).
⁷ M. Grifoni and P. Hänggi, *Phys. Rep.* **304**, 229 (1998).
⁸ M. Holthaus and D. W. Hone, *Phys. Rev. B* **49**, 16605 (1994).
⁹ P. H. Rivera and P. A. Schulz, *Phys. Rev. B* **61**, R7865

(2000).
¹⁰ P. A. Schulz, P. H. Rivera, and N. Studart *Phys. Rev. B* **66**, 195310 (2002)
¹¹ J. M. Villas-Bôas, S. E. Ulloa, and N. Studart, unpublished.
¹² J. M. Villas-Bôas, W. Zhang, S. E. Ulloa, P. H. Rivera, and N. Studart, *Phys. Rev. B* **66**, 085325 (2002).
¹³ C. E. Creffield, *Phys. Rev. B* **67**, 165301 (2003).
¹⁴ P. Domachuk, C. M. de Sterke, J. Wan, and M. M. Dignam, *Phys. Rev. B* **66**, 165313 (2002).
¹⁵ M. M. Dignam and C. M. de Sterke, *Phys. Rev. Lett.* **88**, 046806 (2002).
¹⁶ X.-G. Zhao, *J. Phys. Condens. Matter* **6**, 2751 (1994).
¹⁷ M. Holthaus and D. Hone, *Phys. Rev. B* **47**, 6499 (1993)
¹⁸ From the time evolution, one can see that \tilde{T}_e for the middle/open barrier is $\tilde{T}_e \simeq T_e/80$.